Final Report

Contract Number: DTPH56-15H-CAP07

Prepared for: DOT

Project Title: Electromagnetic Strategies for Locatable Plastic Pipe

Prepared By: The University of Tulsa

Contact Information: Michael W. Keller, mwkeller@utulsa.edu, 918-631-3198

Executive Summary

The goal of the research program presented in this report was to investigate two strategies for fabricating plastic pipe that are intrinsically responsive to electromagnetic interrogation from the surface. The first strategy was to investigate the production of antennas that can be used with either active or passive RFID systems to provide both location and pipe data. The data will provide visibility into the earth without the need for excavation, thereby reducing cost and increasing safety by eliminating the possibility of accidental utility damage. Items such as utility type, depth, and pipe size information will be investigated. Critically, this strategy is focused on fabricating pipe structures in such a way as to produce a continuous production line to ensure cost-effective, locatable, plastic pipe. The second strategy was to incorporate magnetic nanoparticles that will exhibit a strong response to EM radiation from the surface. Two approaches were investigated, a direct incorporation of magnetic nanoparticles and a microencapsulated magnetic nanoparticle approach.

The microencapsulated approach was investigated, but the capsules were found to be insufficiently robust to survive the manufacturing processes associated with PE pipe fabrication. Despite this, Fe-based magnetic nanoparticles were found to be sufficiently robust to survive compression molding. Magnetic testing indicated that the incorporation of these particles significantly increased the magnetic signature of the PE host material and could be a viable route to intrinsically magnetic PE materials.

The antenna approach resulted in the identification of several designs that were viable and was followed up with an in-ground test designed to simulate an in-field utilities location event. Selection of antenna design was performed through combination of open air antenna response testing and simulation. These tests were compared to a baseline control and a delay line-type antenna and a simple bowtie were selected for further testing. Simulated field tests used a ground penetrating radar (GPR) approach and was successful at increasing signal response significantly compared to the baseline control test (empty pipe).

To support this approach, which ultimately was chosen as the more likely path, a new two-phase conductive polyethylene (cPE) material was processed for use as an antenna material. This approach would allow for direct application of antenna structures to the host pipe without the introduction of an external capsule or metallic sheet. Comprehensive mechanical and electrical testing was performed in order to understand the influence of the conductive additive on polymer behavior. This testing included a novel bi-layer specimen that allow for the simulation of pipe deformation with an applied conductive antenna structure. Testing indicated that the conductive polymer could withstand the strains that would be expected during typical pipe handling and installation.

This report is the product of three graduate students Jordan Trewitt (TU), Laura Waldman (TU) and Ravi Venkata (OSU) under the supervision of several Pis Michael W. Keller, The University of Tulsa, Peter Hawrylak, The University of Tulsa, and Raman Singh, Oklahoma State University.

Contents

Chapter 1

INTRODUCTION

Polyethylene offers many advantages over the traditional cast iron for utility lines. For example, polyethylene pipes do not suffer from environmental degradation or corrosion in the way that metals do. Polyethylene is also usually more cost effective than metal, and because of the lower temperatures required for working polyethylene, sections of the pipe can be easily joined together in the field, instead of relying on flanged fittings and mechanical fasteners. Because of these advantages, using polyethylene for storage or transport lines became standard; in 1985 it was estimated that as much as 95% of new utility lines were polyethylene [6], [3], [45], [40].

1.1 Polyethylene Pipe Detection

Traditional utilities pipes are made from metal, such as cast iron or steel. To locate these pipes, workers would use metal detectors or ground penetrating radar (GPR). However, locating thermoplastic pipes, once buried, is difficult, because they cannot

be detected with common electromagnetic techniques. In cities with legacy utility systems, these pipes can be even more difficult to find, because the older metal pipes have a stronger electromagnetic signal than the modern thermoplastic pipes, and there is a higher quantity of buried objects that can reflect radar signals [9]. Knowing the exact location of buried pipes is important, as pipes must be dug up to be serviced or replaced. During construction work, too, the exact location of the pipe must be known so that the pipes are not damaged by equipment. In addition to the main city lines, utility lines run to every house and building. Lines with a diameter larger than 2", by code, must be buried deeper than 24", but even at that depth, the lines are commonly damaged during construction, digging, or even gardening projects. In the case of gas lines, where the contents of the pipe is combustible and under pressure, damage to the pipe can result in explosions [14], [5].

Tracer wires are the most common method of locating polyethylene pipes. Long wires are buried alongside the pipe during installation, at a distance of 6" from the pipe [20]. These wires, which are a continuous conductive source in the ground, can be detected with ground penetrating radar, allowing the operators to understand the location of the pipe. However, these wires commonly corrode or break in the ground, resulting in a wire that can no longer be detected. The wires can also shift away from the pipes, resulting in an inaccurate location. A single tracer wire used for locating multiple pipelines is shown in Figure 1.1 [34].

Starting with a simple underground test, the resistance test measures changes of real DC impedances using high voltage to find large metallic objects or even water sources. This test, however, can be minimized if the conductivity of the soil is not

Figure 1.1: A tracer wire, noted by the arrow, used for locating multiple pipes. [34]

high enough or too high where the current might flow closer to the surface instead of reaching an object. Making matters worse, the object might be too small due to this method's poor resolution. Moving to several kHz, consumer metal detectors operate with two induction coils, one to transmit at several kHz and the other to check the change of the signal, where the operator listens to the change with the audio signal going to headphones. Like the resistance test, they operate better with soil that is relatively moist and conductive with average detection depths of 0.3 m [33]. Conductive pipes, coins and other miscellaneous objects can be easily picked up. However, ground penetrating radar (GPR) has become among the most common methods for locating buried objects, including utility lines. After the radio waves are transmitted, an antenna reflects the waves, after a certain delay, allowing them to be received by the source. Knowing the magnitude of the reflected signal and the time delay, the radar operator can then determine the location of the object

that reflected the waves. In the case of metal pipes buried underground, the GPR is moved along the area of interest and the radio waves are sent into the ground. The metal pipes will function as antennas and reflect strong radar signals, allowing the operators to determine the location of the buried pipes. Because most polymers are naturally nonconductive, the thermoplastic pipes will not function as antennas in the same way. For larger utility lines, the dielectric difference between the pipe and its contents and the surrounding soil is enough so that the location of the pipe can be determined. For smaller pipes, however, their location can not clearly be determined with GPR [10], [9], [52].

1.2 Doped Polyethylene Antenna Approach

If polyethylene pipes could be imparted with the desired electromagnetic properties, they could be more easily detected with ground penetrating radar. One approach is to create antennas from conductive polyethylene, which would provide a clear electromagnetic target for detection with GPR. Polyethylene notoriously resists adhesion, so it is difficult to reliably attach commercial antennas to polyethylene, but an antenna made from polyethylene could be directly and securely molded to the pipe. Because the antennas are made from polyethylene, they would also have the same resistance to environmental corrosion that the polyethylene pipes do.

To make polyethylene suitable for use as an antenna, it has to be made conductive. For antennas in this work, carbon black and aluminum were chosen as the conductive dopants. These materials are more economical than other possible additives, but

still provide good conductivity to the polyethylene. Once the polyethylene had been doped, it could be molded and cut into antennas. However, adding enough dopants to change the electromagnetic properties of the material will change the material properties of the material as well.

During production, thermoplastic pipes are formed through extrusion [3]. Smaller diameter pipes are then coiled onto spools for storage and transport, allowing large lengths of pipe to be transported easily. Larger diameter pipes, however, are cut into 40 foot lengths for transportation [2]. Industry standards dictate the minimum coil size to which a pipe can be bent for installation, to prevent damage or kinking from occurring to the pipe. At the installation site, these pipes can be bent to an even smaller radius before being straightened and installed. During the bending and straightening processes, the polyethylene pipe will undergo strain. An antenna bonded to the surface of a pipe would also have to survive the strains on that pipe, so the antenna material should be well characterized to ensure survivability.

1.3 Magnetic Particle Approach

While the first approach applies antennas made from a conductive material to the pipe after manufacturing, a second approach would impregnate the polyethylene directly with magnetic materials during fabrication. The magnetic materials would allow for the polyethylene to be detectable with metal detectors, similar to legacy metal pipe. Previous work by GTI demonstrates that polyethylene pipes, compounded with up to 24% of a magnetic powder, have been detectable with a hand-held metal

detector at depths of three to five feet [38].

In this work, iron nanoparticles and magnetic ink character recognition (MICR) toner were each molded directly into the polyethylene materials. Because iron will rust at higher rates at the high temperatures required for thermoplastic molding, these materials were also encapsulated in urea-formaldehyde microcapsules to protect the particles from degradation.

For this method to be effective, enough magnetic material would have to be added to the polyethylene to make electromagnetic detection possible. The magnetic materials would also have to maintain their magnetic response so that the pipe could be located over the lifetime of the pipe.

In a future work, the microcapsules could have a core material that would allow for the addition of self healing capabilities to the polyethylene. Thermoplastic healing is usually accomplished through the external application of heat to the damaged area. Capsule-based self healing in thermoplastics has been limited by the high temperatures and high pressures required for molding. For this method to be expanded to include self-healing, the microcapsules would have to have a high enough survivability rate in the polyethylene molding process.

1.4 Antenna Approaches

Some relatively new methods of finding utilities involve using a radio frequency identification (RFID) tag operating in the 100's of kHz, where the user powers the tag and the tag modulates the provided signal. When in use, users place these

tags right above a pipe about every foot or so, injecting useful information onto the tag to indicate the type of utility and the depth. Like tracer wires, these tags are limited to two to three meters, involve using proprietary technologies and readers, are relatively expensive compared to the previous solutions and are slated to last 20 to 40 years due to constraints in memory technology on the RFID chip [1]. On the other end of the frequency spectrum, is the ground penetrating radar (GPR) technology. Like traditional radar, GPR sends out a pulse and waits to hear how that signal has changed over time. Unlike near field methods mentioned before, how well this technology works depends on the far field attenuation being several magnitudes greater than free space loss thus determining maximum penetration depth, and dielectric constant slowing down the speed of light. Additionally, ground clutter distorts signals from the GPR caused by small voids in the dirt and gravel [64]. Interpretation of the data is critical, in this case, is critical while compiling the scans to indicate the three dimensional location of the object, so a GPR is only as good as its user or even its interface [13]. Luckily, GPR can detect both conductive objects and changes in dielectric constant. However these technologies depend on their own specialized equipment to find objects of interest in the ground.

1.5 Research Objectives

The research presented in this reports focuses on two primary objectives. The first is to fabricate polyethylene that is sufficiently electromagnetically active to be detectable using GPR or similar approach. The second objective is focused

developing simple artificial tags that are attached or incorporated onto underground objects to distinguish themselves from other natural objects more readily using a GPR or other radar systems. The idea behind this, is not to create new test equipment, but instead to create something unique and not seen otherwise, using the above mentioned methods. Specific objectives were

- Process and characterize conductive polyethylene materials.
- Determine influence of any applied conductive material on the mechanical performance of the underlying PE pipe structure.
- Investigate varying technologies that might be used to find underground objects to select candidates for simulation and experimentation.
- Simulate how differing environments affect transmission lines and antennas designs to identify suitable candidates for experimentation.
- Build and manufacture tags in a cost effective manner so that tags do not outweigh the cost of the object buried.
- Conduct experiments to verify how environments affect antennas and to test tags in free space and soil to determine suitability in locating utility pipelines.

Chapter 2

Radio-based location of structures in sub-optimal conditions

In recent years, two separate, but similar applications have been maturing without being combined into each other. First, the use of ground penetrating radar (GPR) to find an endless number buried objects and second, the use of ultra wide band (UWB) tags to identify objects of interest, usually in the retail or inventory environments. The reason behind why these two have not hybridized might be threefold: regulations with UWB, the dilemma of electromagnetic attenuation and the market not knowing some of its needs.

UWB tags in logistics and retail environments have been subject to the FCC's part 15 ruling and other European standards since 2002, confining UWB technologies to S, C and X bands. However GPRs fall under more relaxed standards since the energy from the pulse dissipates into the ground instead of propagating into free space

where interference can be a problem and simply because GPRs are not a consumer product in high use. These standards indicate that a GPR cannot emit above certain specified of energy so many meters away and that GPR's center frequency must be below 10 GHz. Because of the limiting frequencies for the former UWB tags, these cannot be used in the attenuating environment of underground utilities with detection limits of around 0.25 m. However, the principals for UWB tag design should remain the same when shifting the center frequencies of these tags below 1 GHz allowing commercial GPRs to detect the tags in question. The same electromagnetic principles for smaller tags in the microwave regions carry over for larger tags in the VHF and UHF regions. If this was any other situation involving microwaves the reverse would normally be true; radio technologies at lower frequencies are scaled to higher frequencies as equipment improves.

2.1 Intentional Detection Methods of Passive Systems

Although it is true that various radars can detect objects with large enough cross sections, these objects become harder to recognize if they reside in cluttered and dispersive environments. Therefore, to aid in recognition, varying forms of tags can be added to underground objects, where the signal emanating from the object can become easier to isolate and further information about the object could be added. Three main approaches exist for locating tags by: modulating incoming signals, delaying incoming signals or varying the frequency response back to the system. Different aspects of these methods can be combined, to create an even more robust

design. Yet all designs will exhibit some common characteristics where both may act similarly through different means. For example, all methods have to connect to antennas that receive and transmit an incoming signal.

2.1.1 "Dumb" Chip Based RFID

Chip based RFID tags can be further divided into two separate groups: those that have complex circuitry like near and far field tags that are able to modulate data from an integrator's continuous signal. This type is unlike other chip based tags like harmonic based tags with a small number of components. However, the more complex RFID tags carry more information with stored memory and are rated for 20 to 40 years as mentioned earlier and additionally, RFID tags with batteries have longer detection ranges with battery lives of two to four years [47]. Still because these utility pipes need to operate for possibly 100's of years these smarter RFID tags will not be included in this review as they do not fit within the requirements well.

Harmonic Nonlinear Radar

The first and simplest chip based design by far, is the harmonic nonlinear tag. This tag only relies on a single diode. Commonly used in frequency multipliers, the Schottky diode, used in these tags, produces harmonics of the input frequency. Although objects naturally produce harmonics from incident continuous waves, the Schottky diode generates harmonics magnitudes larger than the former. The basic idea behind a harmonic tag goes back to Augenblick in 1969, where he describes the

frequency doubling tag as well as the needed transmitter and receiver [17]. When using a harmonic radar, the receiver and transmitter have to be further isolated with high order bandpass filters, since transmitters also produce harmonic frequencies due to the nonlinear elements needed to generate and amplify the output signal. Even though these tags lack any form of data storage, they still can outperform RFID chips because of sheer simplicity.

Surface Acoustic Wave (SAW) ICs

The second chip based tag is a slightly more complex IC, which is the SAW chip. SAW ICs are based off of a piezoelectric effect where an electric wave is effectively converted to an acoustic wave with a certain degree of conversion loss [23]. Their first use case is to delay a signal by several milliseconds, but they can also be used effectively as filters. To create an ID, several delay lines are used to have on and off stages at certain times as described in Edmonson's patent [25]. Friedt also uses surface acoustic wave (SAW) ICs to hold up the antenna mode scattering by several microseconds thus indicating whether a tag was underneath 5 m of snow [28]. These types of time delay tags would be able to be detected with commercially available GPRs. The biggest limitation to these chips is the availability and price of each IC.

2.1.2 Chipless Based RFID

Due to some limiting factors of costs and power of chip based RFID tags, many chipless based RFID tags are designed to operate within the FCC's Part 15 UWB spectrum ruling classifying use from 3.1 to 10.6 GHz operating with an Equivalent

Isotropically Radiated Power (EIRP) of -41.3 dBm/MHz [24]. However, there seems to be a lack of research with some of these types of technologies in conjunction with GPRs in the VHF and UHF spectra, which can outperform in terms of distance due to previous mentions of attenuation at higher frequencies [9].

Transmission Line Delay

The first type of chipless based tag is a transmission line tag. In practice, this type of tag uses the transmission line to delay a signal by several nano seconds. This signal is either reflected at the end of the transmission line to be re-transmitted into the same antenna or is passed through to another antenna. As Dardari notes, transmission line tags reveals two types of reflections: structural scatter or typically known as the radar cross section (RCS) and antenna mode scattering coming from the delay line pulse [22]. With a single antenna tag, an antenna connects to a transmission line where after some length the transmission line is either terminated with an open or closed circuit with the ground plane as noted by both Hu and Dardari [32, 22]. Dey continues to develop this tag re-purposing uses the same transmission line delay tags to indicate whether or not a crack occurred, such that the delay line shortens when the line breaks [23]. Transmission line delay tags could possibly exhibit their usefulness to aid in recognition with GPR scans by varying forms of the tags on underground objects.

Cross Polarization

A variation of the transmission line tag, is the second type of chipless based tag, the cross polarization tag. A cross polarized (CP) tag involves two perpendicular antennas. These types of tags operate with both pulsed time domain radars and frequency based radars. For an infinitesimally small wire, there should be perfect isolation between a horizontally polarized and vertically polarized antennas, but practically Adamiuk found that there is around -20 dB of isolation with polarization mismatch between two perpendicular antennas close to each other [11]. The cross polarized tags will already present a small time delay similar to the previous tags, where Shen used a circularly polarized antenna connected to transmission lines with open and short circuits, such that the receive antennas and transmit antennas were linear polarized and isolated by the change in polarization from vertically polarized when transmitting and horizontally polarized when receiving [56]. Using polarimetric radar, C. Feng even uses two simple dipoles rotated at varying angles to record 3 bits of information per tag [26]. Even innovative polarimetric GPR setups, that X. Feng uses, would also work well with the cross polarized tag when it records the response of all polarizations over different passes [27].

Frequency Selective

To build upon the transmission line tag, is the third type of chipless based tag, the frequency selective tag. Frequency selective tags are by far the most common type of UWB chipless tag in the C and X bands, because of their ability to hold large amounts of data if seen through something like a vector network analyzer (VNA). Because of

the nature of these tags, most tags have to be isolated with cross polarization when the transmitting signal does not overwhelm the underlying response from the tag [41, 49, 63]. Nijas' tag used quarter wave resonators with a microstrip to create an 8-bit tag [41]. Similarly Preradovic, used spiral resonators on a microstrip to create multibit tags, such that short a resonator to change a bit from 1 to 0 [49]. Weng presents a unique way to reduce the cost of these tags with a single layer coplanar waveguide (CPW), using in line resonators to create stop band responses [63]. Dey presents two more types of frequency selective tags where the frequency response from resonators vary according to either the temperature or humidity [23].

Characteristic Mode

A variation of the frequency selective tag and the fourth type of chipless tag is the characteristic mode tag. To simplify designs even more, characteristic mode antennas act like inductor capacitor resonators with low dampening factors, such that if a pulse excites the tag, it resonates at a set frequency. In a continuous wave case, these kinds of features are similar to a backwards propagating meta material that can create flat parabolic arrays or invisibility cloaks. Rezaiesarlak uses this feature in several 4-bit tags, such that when the diameter of the arc of the tags changes, the resonant frequency also changes [50]. Vena uses this feature in resonators printed on paper such that the tags would have at most around 20 bits of information on them [60].

2.2 Electromagnetic Propagation in Problematic Environments

Propagation is directly related to the transmission coefficient that is the S21 parameter in a two port system. In a coaxial line, there are known values for losses over large distances at varying frequencies and known propagation speeds. In point to point over-the-air transmission, there are free space losses over distance and the wave travels at the speed of light. However, when looking at a comparison of link budgets, transmission through subterranean mediums can be more difficult than in some deep space communication applications like lunar landers.

Working in underground environments increases the issues not seen in free space propagation. Soil, having dielectric constants higher than one, biases antennas and changes impedances of transmission lines in contact with it. Soil would also be inconsistent, that is having varying layers of dielectric constants and conductivities that can change with the weather, thus increasing the chance for a reflection just from a change in soil. This can either be due to changes in the material changes in the soil such as moving from clay to sand or to gradients in moisture levels. Due to conductivity and permeability, from an increased iron content in some soils, signal attenuation can be several orders of magnitude higher than free space. Liu and others covers the details of relative dielectric constants, phase velocities and attenuation values transmission for common materials [51].

2.2.1 Antennas

To over-simplify, antennas are impedance transformers, that is antennas act as an intermediary between the impedance of the transmission line and the impedance of the surrounding space, whether free space or soil. This section will review some antenna designs from simple to UWB deriving back to how Schantz goes through the history and science of UWB antenna theory [55]. Although antenna theory and design is useful as a basis, Chapter 3 will expand upon potential antennas with simulations.

Dipole Antennas

The simplest of antennas is the dipole antenna or more specifically the half-wave dipole. It consists of two wires, or elements, where one connects to the ground and conductor of the transmission line. The length of each element determines the frequency at which the antenna resonates such that:

$$l = \lambda/4 \tag{2.1}$$

Bowtie Antennas

The best explanation for bowtie antennas is that "fatter is better." Increasing the width of an element on a dipole increases bandwidth, up to a certain point. Early researchers found that these antennas can obtain higher bandwidths, if the fatter dipole elements are instead triangles, it can form an antenna that looks like a bowtie. Since the dawn of radio, these antennas have been more commonly used in the form

of biconical antennas. If the triangle were to extend into an infinite length, it would theoretically have infinite bandwidth.

Circular Planar Antennas

The circular planar antenna continues the idea of the bowtie antenna, save for instead of triangles, circles are used instead. Although these antennas act like dipoles at lower frequencies, they become more directional towards the higher end of their frequency bandwidth. This directionality feature precedes Vivaldi antennas which would instead use exponential tapers instead of these circular tapers.

Antennas in Dielectrics and Lossy Mediums

The way antennas react to dielectrics relates to the speed of an electromagnetic wave through any dielectric medium as in Eq. 2.2. As a dielectric constant increases, the speed of the electromagnetic wave slows down. When the speed of the electromagnetic wave slows down, it means that for the same frequency, the wavelength becomes shorter as the dielectric constant increases. Many times, designers use this to create smaller antennas, but at other times can plague antenna engineers if they do not know what the application environment for an antenna is.

$$v = \frac{c}{\sqrt{\epsilon_{eff}}} \tag{2.2}$$

In particular interest is dielectric half spaces. These spaces are defined as the border between dielectric environments, most commonly bordering free space. The apparent dielectric constant at this border is simply the average between the two,

where the best case is defined in Eq. 2.3. Antenna patterns placed on this half space bias heavily towards the stronger of the two dielectrics [29].

$$\epsilon_{avg} = \frac{\epsilon_1 + \epsilon_2}{2} \tag{2.3}$$

Transmission Lines

Transmission lines act as a means to transport energy with minimal transmission losses defined by specific impedances that are determined by the line's intrinsic capacitance and inductance. Of particular interest, microstrip and CPW transmission lines carry energy over conductively clad dielectric substrates. Microstrips consist of two conductive layers, where one acts as a ground plane and the other as which also acts as a specific impedance. These transmission lines, however, only need a single conductive layer of width w, where the a gap of width s separates the conductor and ground plane. More desirably, CPWs may also use another ground plane below the main conductor, acting more like striplines having two modes where it acts like a CPW without a ground plane and a microstrip line. A single layer can also be desirable when ease or cost of manufacturing necessitates itself like in many current RFID tags made from a single layer of aluminum foil or those that are printed. In both CPWs and microstrips, the phase velocity of an electromagnetic wave is determined by the effective substrate dielectric constant that comes from the substrate dielectric constant and the surrounding material, where the speed is determined by Eq. 2.2.

Although the surrounding material is assumed to be free space, there are cases

where there are other surrounding dielectrics or even a metal cover might be above the microstrip or CPW. Surrounding dielectrics affect CPWs without ground planes more than microstrips due to couplings between the ground and line. Metal covers, if close enough, might cause the microstrip or CPW to act like a stripline. The difference between microstrips and CPWs is simple. With microstrips, the ground is either below the conductor separated by a substrate. Conversely with CPWs, the ground plane is on either side of the conductor. If needed a CPW can also have a ground plane beneath the conductor, but this results in the same expense as a microstrip. CPWs can be printed with conductive ink and cut out of thin conductive foils fairly easily. Steer [57] makes a note of the effective dielectric constant from the equations from Hammerstad where the effective approximate dielectric in free space for a microstrip is determined by Eq. 2.4, where h is the substrate height and w is the conductor width [31, 30].

$$\epsilon_{effmicrostrip} = \frac{\epsilon_{substrate}+1}{2} + \frac{\epsilon_{substrate}-1}{2}\frac{1}{\sqrt{1+\frac{12h}{w}}} \tag{2.4}$$

Similarly the effective dielectric of a CPW with a ground plane in free space is just as complicated in Eq. 2.5 and 2.6 where s is the separation of the ground plane from the conductor.

$$\begin{aligned}\epsilon_{CPW} = 0.5(\epsilon_{sub}+1)\tanh[1.785\log(\frac{h}{s})+1.75]+ \\ \frac{ks}{h}[0.004-0.7k+0.01(\epsilon_{sub}+1)(0.25+k)]\end{aligned} \tag{2.5}$$

$$k = \frac{w}{w+2s} \tag{2.6}$$

However, when without a ground plane, the CPW's effective dielectric constant is simple as Rosu notes it is the average of the two dielectrics, assuming large enough substrates and not just for free space in Eq. 2.7 [53].

$$\epsilon_{effCPW} = \frac{\epsilon_{substrate} + \epsilon_{environment}}{2} \tag{2.7}$$

The combination of these transmission lines and antennas produce the basis behind time delay tags. When simulating and testing, the results will make more sense when seen through this understanding of the elements and half-spaces.

2.2.2 Limitations on Dumb Tags

A dumb tag is seen as a type of tag without active elements which can be seen more as passive. In this regard, a dumb tag's identity is hard to change as it can only be modified through largely mechanical means. Assuming the price of antennas for all of these tags is the same price, the characteristic mode tags will be the cheapest. This is followed by the frequency selective and transmission line tag which will use more substrate area. Since the cross polarization tags requires the use of two antennas,substrate area and therefore cost should be about twice as much. Harmonic based tags typically use the same setup as cross polarization tags, so cost just as much as that plus the cost of a diode that might be several cents. The price of a SAW IC dwarfs the cost of any antenna, where one might cost ten's of cents versus several dollars respectively.

Regarding the viability of these tags in a dielectric environment, some tags

can change their characteristics. The first two chip based tags, the harmonic and SAW tag, do not change how they act. The harmonic tag will always double the input frequency. The SAW tag is isolated within its own package that neither the delay type characteristics nor frequency characteristics change. The only thing that changes with both of these is matching networks which can determine reflection characteristics. The chipless based tags, the transmission line delay tags will vary with time delay, however for the frequency based tags, the center frequency would decrease. For the characteristic mode tags, if the soil has any conductivity, the dampening factor of these tags increases and they might not resonate. The only tag that would not be affected at all, is cross polarization tags, since it's only based off of the antennas and can match to itself.

Additionally there are several tag density issues with these tags. Unlike many of the smarter tags from Impinj or 3M, these former dumb tags never turn off where the interrogator always sees the tags. In typical chip based RFID tags, the chip will listen for a randomly generated ID and once the reader finishes with the tag, it will cycle off until the power is reset. This process allows a larger number of tags can operate in a smaller area. Hu notes that errors in delay line tags increase as the number of tags increases [32]. Similarly, Barton in a NASA report, noted that SAW tags, which are somewhat similar to delay line and frequency selective tags, noted that SAW tags have limits on information capacity and collision resolution [18]. This correlates with what Vena mentioned the limits of the characteristic mode tags, where it was limited by the bandwidth of the interrogator [60]. Some of these limitations can be relieved when wider bandwidths are used though.

The dumb tag presents the easiest and fastest way to experiment without using proprietary technology or vastly more complicated methods. This route should also be able to complete a minimum viable product that fits within the specification and goals of this thesis.

Chapter 3

Experimental Methods - Doped Polyethylene

Antennas made of a conductive polyethylene would allow for the pipes to be more easily detected with ground penetrating radar by providing an electromagnetic target. Unlike commercial time delay antennas, these polyethylene antennas could be directly molded to the polyethylene pipe. A material used for antennas must have sufficient conductivity to provide a strong electromagnetic response during detection, so the polyethylene is doped with quantities of conductive additives and then molded into antenna shapes. For these antennas to be a long term solution to the problem of pipe location, the antenna material must be able to survive the deformations experienced by the pipe throughout its lifetime, especially during transportation and installation, when the strains are higher than in normal service.

3.1 Materials and Mixing Procedure

The percolation limit refers to the point at which enough of an additive has been added to a material such that there is a continuous path between the particles of the additive. To make an effective conductor, the dopants must be added to the polyethylene matrix in amounts over the percolation limit, such that a continuous conductive path exists in the polyethylene. In this work, carbon black and aluminum flake were chosen as the primary dopants. Carbon black was chosen as an additive because of its low cost and its large surface area-to-volume ratio, so that it might allow for a continuous path through the material. Aluminum flake was chosen because the bulk aluminum would lower the overall resistance of the material. Additionally, both of these materials are more economical than other materials which may have a higher conductivity, an important factor given the quantity of polyethylene pipes in service.

Doped polyethylenes were made with up to 15% of carbon black and up to 10% of aluminum flake by volume. The materials were compounded with a Banbury mixer located in the Mechanics of Advanced Materials Lab at OSU-Tulsa. The polyethylene was heated to melt at 160°C for at least five minutes, and then dopants were added and combined with a mixer speed of 12 RPM for a minimum of fifteen minutes. The resulting plastic was then compression molded to the desired thickness with a press heated to an average of 170°C [45], [16]. The mixing process is shown in Figure 3.1.

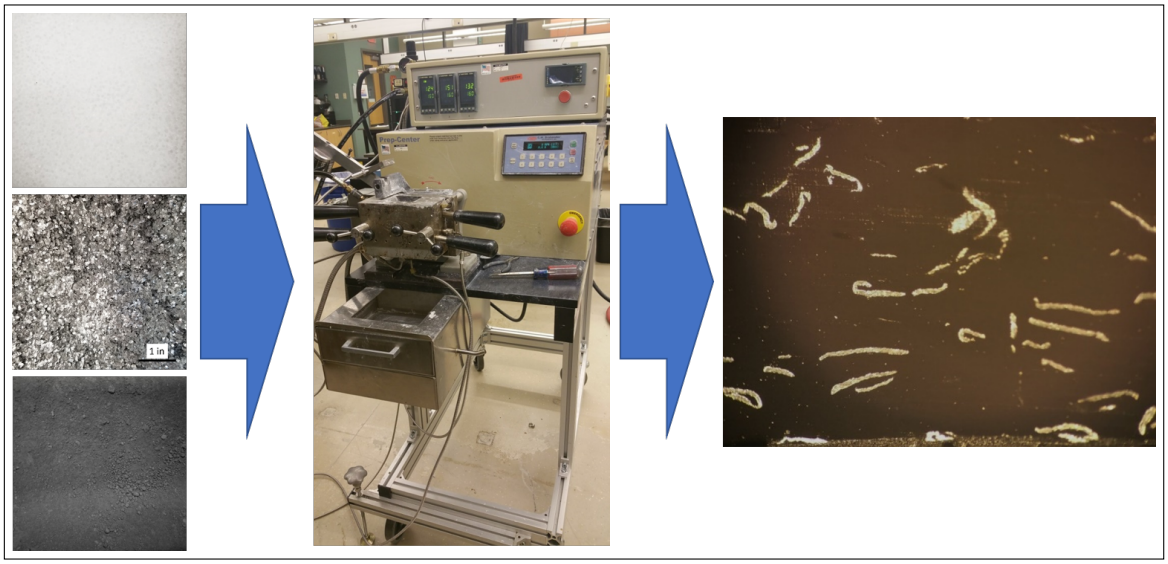

Figure 3.1: Schematic of the process for mixing dopants into polyethylene. On the left are the constituent materials, central is the mixer, and on the right is a cross section of the finished material.

3.2 Electromagnetic Properties Testing

3.2.1 Resistivity of Doped Polyethylene

To determine which of the additives had a larger effect on the conductivity of the material, the percentage of one dopant that was added to polyethylene was varied while the other was held constant. Even at high volume percents, the large flakes of the aluminum did not form a continuous path when mixed into the polyethylene. The smaller carbon black particles could be evenly distributed throughout the polyethylene matrix, creating the continuous electrical path necessary. Without carbon black in the polyethylene matrix, there was no conductive path through the polyethylene, and so all tested materials contained at least 5% carbon black. The aluminum flake, when

added to the carbon-doped polyethylene, served to further lower the bulk resistivity of the polyethylene composite.

Rectangular samples were molded from the various doped polyethylenes, then sectioned with a Buehler Iso-Met 1000 diamond saw to create samples that were approximately 1" in length and width and 1/4" thick. These samples were polished with successively finer grits of sandpaper and finally a felt pad. Samples were clamped between two aluminum plates and resistance was measured across the plates to get a through-thickness measurement.

3.2.2 Doped Polyethylene Antennas

Once a material was created with a low enough resistance, an antenna was created out of the material to determine if a polyethylene antenna could be detected using ground penetrating radar. A plate of the doped polyethylene material was molded, then a bowtie antenna was cut from the plate using an Epilog 40 W laser cutter. Similar bowtie antennas were cut from steel foil, also using the laser cutter. A cross polarization antenna was chosen as the performance baseline and was cut from aluminum foil using a vinyl cutter. The antennas used can be seen in Figure 3.2.

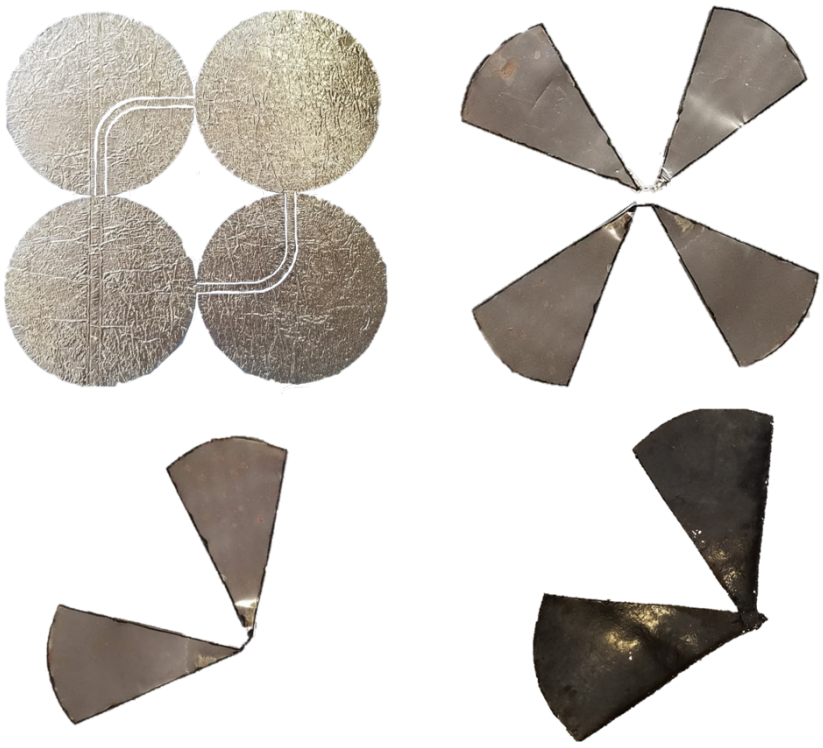

Figure 3.2: Antennas used in the GPR test. Clockwise from top left: Aluminum cross-polarization antenna, steel double bowtie antenna, doped polyethylene bowtie antenna, steel bowtie antenna.

3.3 Material Properties Testing

3.3.1 Tensile Specimens

A material used for antennas that will be bonded to pipe should be able to survive the strains that the pipe will experience during transport and installation. To determine the material properties of the doped polyethylene material, tensile tests were performed according to ASTM Standard D 638: Standard Test Method for Tensile Properties of Plastics [8].

Tensile tests were performed on both neat and doped polyethylene specimens, to quantify the change in material properties due to the addition of the conductive dopants. Plates were molded to 1/8" and ASTM Type IV specimens were cut out of the plates with a specimen press.

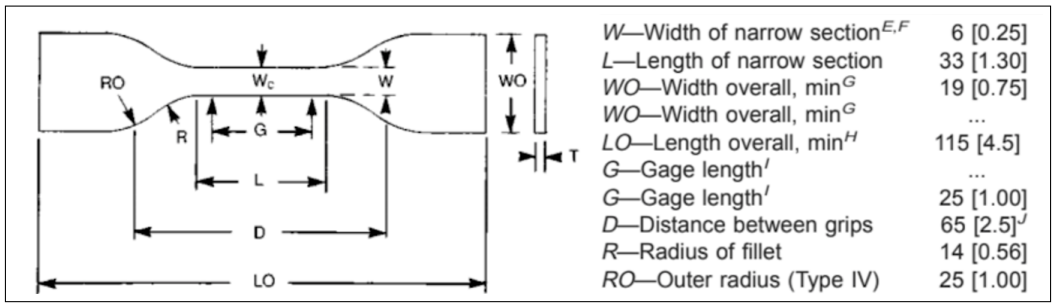

Figure 3.3: Dimensions of an ASTM Type IV tensile specimen. Units are mm [in] [8].

3.3.2 Bilayer Tensile Specimens

Tensile tests were performed with samples consisting of layers of both the neat and doped polyethylene molded together, to determine how the properties of the material

would change if antenna structures were molded to a pipe. Sheets of both doped and neat polyethylene were molded, then Type IV specimens were cut using a specimen press. These samples were molded together with wires in between the layers of polyethylene so resistance could be measured across the specimen. The specimens were then milled back to specified dimensions.

For the bilayered specimens, a multimeter was set up to record the resistance and report that value along with the load and displacement measured by the load frame. When the resistance grew to infinity, it signified that the conductive material had separated and would no longer pass a current. The experimental setup for this test is shown in Figure 3.4.

Following testing, representative fracture surfaces of all the materials were examined with an optical microscope and with a scanning electron microscope (SEM). The scanning electron microscope requires that specimens be conductive, but the conductivity of the doped polyethylene is insufficient. Tensile specimens were sectioned so that the fracture surfaces could be attached to SEM specimen mounts with conductive glue, then sputter coated with a platinum-iridium target to form a conductive layer on the specimens prior to imaging.

3.3.3 Fracture Toughness

To determine how adding quantities of dopants to polyethylene affected its ability to resist crack growth under load, fracture toughness tests were performed on both the neat and doped polyethylenes. Single edge notch beam (SENB) specimens were created by molding polyethylene pellet in a mold with rounded rectangular slots

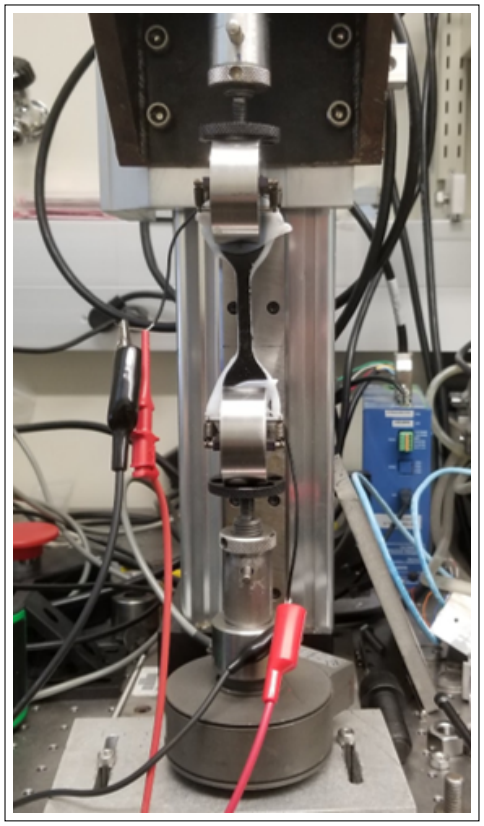

Figure 3.4: Experimental setup for the bilayer polyethylene tensile tests.

and then slicing the rectangular bricks to create two specimens of correct proportion from each mold. The specimens were then pre-cut with a diamond sectioning saw and then the crack was sharpened using a razorblade. After the samples were prepared, the samples were loaded in a load frame with a three-point bend fixture. The dimensions of the specimens, as seen in Figure 3.5, the dimensions of the test fixture, and the procedure for crack cutting and sharpening were dictated by ASTM D 5045: Standard Test Methods for Plane-Strain Fracture Toughness and Strain Energy Release [7].

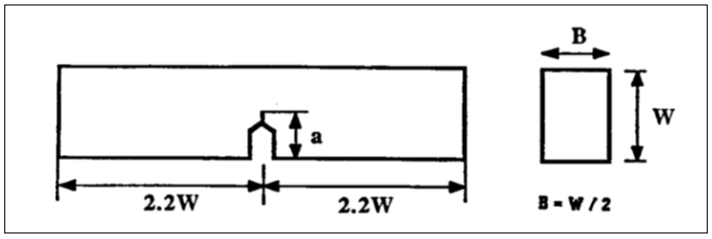

Figure 3.5: A schematic of a single edge notch beam specimen used in a three-point bend test. The crack length a should be such that $0.45 < a/w < 0.55$ [7].

Fracture toughness is calculated with Equation 3.1 [7].

$$K_{IC} = \frac{P}{BW^{1/2}} f(x) \tag{3.1}$$

In this equation, P is the load, B is the specimen thickness, W is the width of the specimen, and a is the length of the crack. The function $f(x)$ is shown in Equation 3.2, and x is shown in Equation 3.3.

$$f(x) = 6x^{1/2} \frac{1.99 - x(1-x)(2.15 - 3.93x + 2.7x^2)}{(1+2x)(1-x)^{3/2}} \tag{3.2}$$

$$x = \frac{a}{w} \tag{3.3}$$

3.4 Pipe Strain

Polyethylene pipes are often coiled on large spools for transport, and then straightened for installation underground. The act of coiling these pipes causes strains in the polyethylene, and so any antenna that has been applied to the pipe should be able to survive these strains.

The maximum strain that will occur on a pipe is on the outer surface of the pipe when the pipe is bent to the smallest radius. Industry standards dictate the minimum bend radius to which a pipe can be bent. This bend radius is a function of the dimension ratio (DR), which is the ratio of the wall thickness to the outer diameter of the pipe [4] [5]. Polyethylene pipes are classified by this dimension ratio, which is similar to a schedule rating for other types of pipe. A lower DR indicates a larger wall thickness, which in turn corresponds to a higher pressure rating for the pipe. A pipe with a higher dimension ratio can also have a smaller minimum bend radius. Bend radius is calculated by multiplying the bend ratio for a given DR with the outer diameter of the pipe, as shown in Equation 3.4 [15].

$$\rho = \alpha * D \tag{3.4}$$

In this equation, ρ is the radius of curvature of the pipe, α is the bend ratio, and D is the outer diameter of the pipe.

Given the bend radius of a pipe, the maximum strain on that pipe can be calculated with Equation 3.5 [39].

$$\epsilon = \frac{t}{D}\frac{3\frac{\Delta y}{D}}{1-2\frac{\Delta y}{D}} \tag{3.5}$$

Δy is the vertical change in the diameter of the pipe and t is the wall thickness of the pipe. The quantity $\frac{\Delta y}{D}$ can be calculated with the equation shown in Equation 3.6 [39].

$$\frac{\Delta y}{D} = \frac{1}{16}\frac{D^2}{t}\frac{D^2}{\rho} \tag{3.6}$$

The calculated strains for a nominal 1" pipe are presented in Table 3.1. Appendix 11.1 contains calculated strains for a larger variety of pipe sizes and dimension ratios.

Table 3.1: Strains on a 1" pipe of varying dimension ratios [15].

DR	Wall	Bend Ratio	Long Term Minimum Bend Radius	Strain
7	0.188	20	26.3	0.145%
9	0.146	20	26.3	0.187%
11	0.120	25	32.875	0.146%

However, pipes can be bent to a tighter diameter for short-term applications such as transportation or installation. Though the diameter of this coil will be smaller than the long term minimum, the coil must still be wide enough to prevent kinking. The minimum short term bend ratio defines the tightest bend that the pipe should

experience. The highest strains that the pipe would experience are on the surface during this short term bending. Calculated strains are shown in Table 3.2. Note that although the bend ratio was decreased by a factor of two, the strains increased by an order of magnitude.

Table 3.2: Strains on a 1" pipe of varying dimension ratios for short term bending [46] .

DR	Wall	Bend Ratio	Short Term Minimum Bend Radius	Strain
7	0.188	10	13.15	1.397%
9	0.146	10	13.15	1.879%
11	0.120	13	17.10	1.334%

Calculated strains were experimentally verified using digital image correlation (DIC). A 1" nominal pipe with DR 11 was speckle patterned using spray paint. A wooden fixture was created so that the pipe could be fixed at one end and bent over a wooden mandrel with a constant radius. Wooden mandrels were made with the minimum install radius of 32", 23.5", and the minimum short term bend radius of 17". Locating pins ensured that the placement of the wooden arcs was repeatable. The pipe bending test fixture and a schematic of the setup can be seen in Figure 3.6.

Before the test, the polyethylene pipe was fitted over a steel pipe to straighten the pipe. This represented the initial reference point for the pipe. The steel pipe was then removed and the polyethylene pipe was bent over the mandrel, and the final images were taken. The strains were then calculated with DIC software.

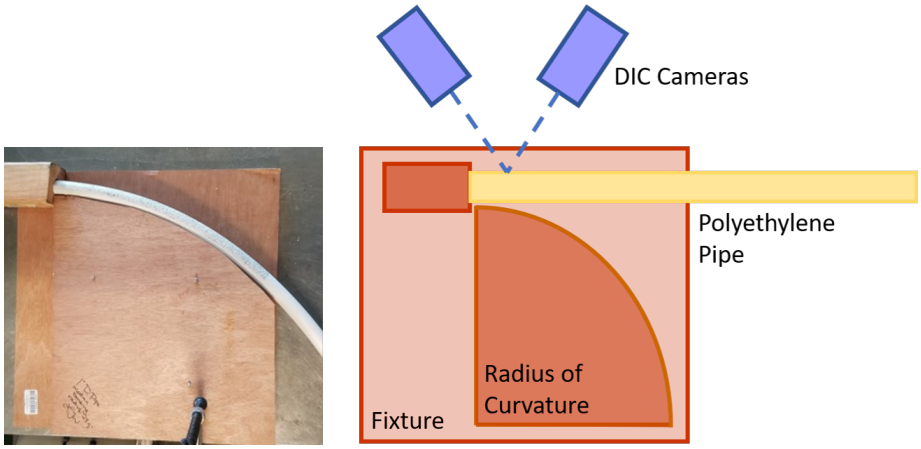

Figure 3.6: (Left) Test fixture and (right) schematic of the setup for a pipe bending test.

Chapter 4

Characterization of Doped Polyethylene

4.1 Electromagnetic Properties of Doped Polyethylene

4.1.1 Resistivity of Doped Polyethylene

The most effective material for antennas will have the highest conductivity so that the least energy is lost to heat within the antenna. An electromagnetically active composite polyethylene was created by compounding conductive fillers into polyethylene. Conductive fillers in a matrix have a percolation limit, at which point a network of filler particles has been established through the matrix, and additional filler will not continue to raise the conductivity of the composite. Carbon black is commonly used as a conductive filler in thermoplastics due to its economy and ease of compounding. Previous studies have shown that, depending on the size and aspect ratio of the filler

particles, percolation of carbon fillers in polyethylene occurs between 5-40%. The conductivity of a composite can be increased beyond the percolation limit through the addition of a second filler with a different aspect ratio, which can bridge areas of high conductivity. This third phase will also have a percolation limit within the composite.

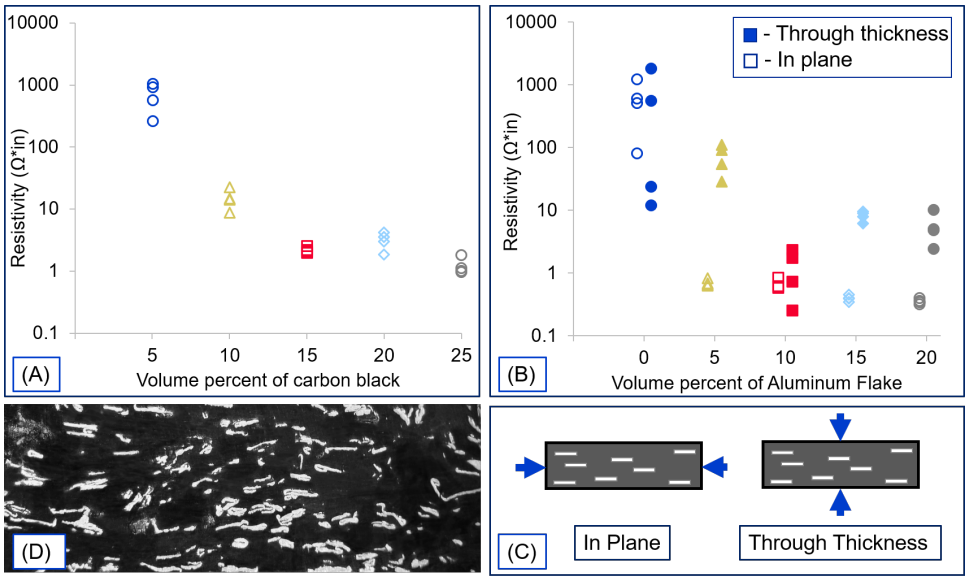

Figure 4.1: a) Resistivity of conductive polyethylene containing only carbon black as filler. (b) Resistivity of conductive polyethylene containing both carbon black and aluminum as fillers. (c) Schematic of resistivity measurements. (d) Cross-section of conductive polyethylene with both carbon black and aluminum.

The carbon black used in this study reaches percolation at 15% in polyethylene. To further increase the conductivity of the composite material, aluminum flake was also compounded into the material. During manufacturing, the aluminum flakes become aligned with the plane of the material, as seen in Fig. 4.1d. The alignment of flake within the material causes anisotropy in the conductivity of the material.

Resistivity for a three phase composite with polyethylene, 5% carbon black, and increasing aluminum flake was measured to determine the percolation limit for the aluminum flake in the conductive polyethylene matrix. Resistivities for a composite with a particular loading are shown in Figure 4. For each loading, the dataset on the left represents measurement in the plane of the material, and the dataset on the right represents measurement through the thickness of the material, as shown in Fig. 4.1b. For a composite material with only carbon black and no aluminum, there is no statistical difference between the resistivity measurements in either direction. When measured through the thickness of the material, the aluminum reached percolation at 10% loading. However, when measured in the plane of the material, the aluminum flake reaches percolation at 5% and has a lower overall resistivity than the material with 15% carbon black in the matrix. The aluminum flakes provide longer conductive paths in the plane of the material due to their alignment. In the case of antennas, this alignment would provide lower resistance in the direction of current flow, resulting in more efficient antennas than if the aluminum flakes were not aligned, or aligned in the transverse direction.

4.2 Dielectric Property Characterization

Ground penetrating radar signals are reflected by the differences in dielectric properties of adjacent materials in the area of interest. To predict how electroactive polyethylene will behave in service, its dielectric constant, or permittivity, should be characterized. The simplest standard measurement techniques for measuring the electrical permittivity

of materials involve creating capacitors from the material and measuring the time constant of a circuit made with the capacitor. However, these methods are not valid at the higher frequencies that are used for ground penetrating radar applications. Instead, a calibration tool called a precision airline is used to test a sample of the material with a network analyzer. The airline is a sample holder with a calibrated rod that runs through its center. A hollow cylindrical sample of the material under test is inserted in the airline with the calibrated rod through the sample. The airline can then be connected to the network analyzer which will report the scattering parameters of the setup, which can be used to calculate the permittivity, similar to how the antenna resonant frequencies are measured. The airline connected to the network analyzer is shown in Figure 4.2.

The airline requires samples of test material that are long, thin hollow cylinders, with outer diameters of 7 mm and inner diameters of 3 mm. Because of the brittleness of the composite polyethylene, these samples must be molded, and cannot be machined. A dimensioned drawing of the custom mold is shown in Figure 4.3, and the completed mold is shown in Figure 4.4. During the sample manufacturing process, two identical molds will be used to compression mold the cylindrical samples required for permittivity measurement with the airline. Specimens produced with this mold are shown in Figure 4.5.

After manufacturing, the tube specimens were inserted into the network analyzer and the scattering parameters of the material were measured. ASTM Standard D 5568 outlines a procedure for measuring frequency dependent permittivity using The Nicolson-Ross-Weir method. Permittivity is a relative measurement, and so

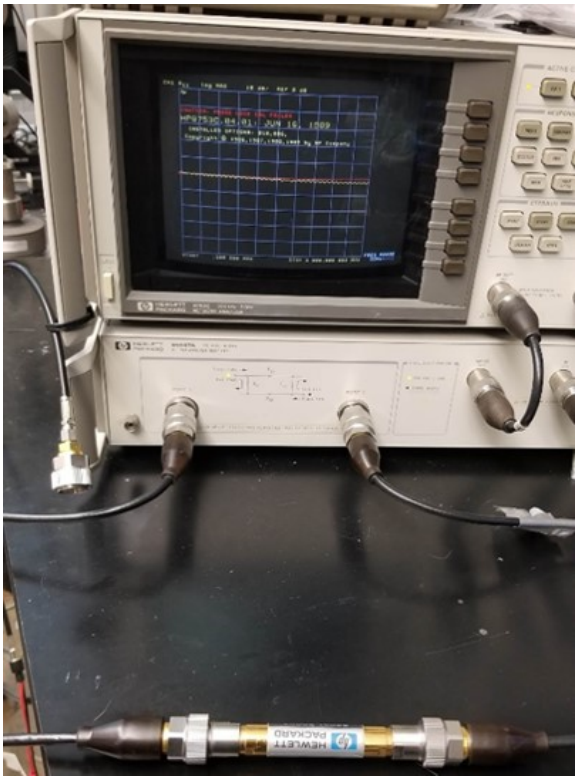

Figure 4.2: The airline connected to the network analyzer.

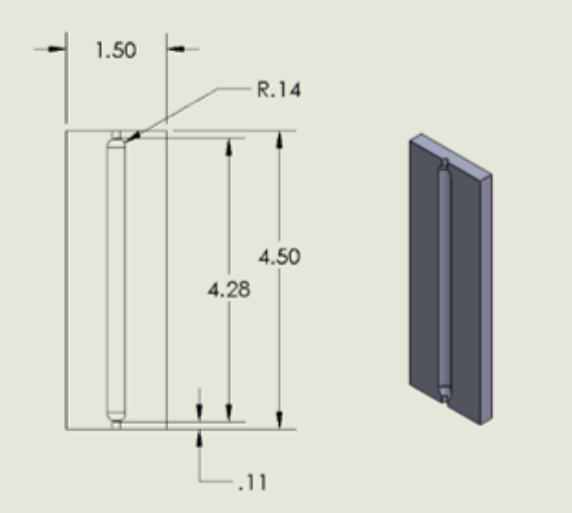

Figure 4.3: A dimensioned drawing of the mold that will be used to create polyethylene specimens.

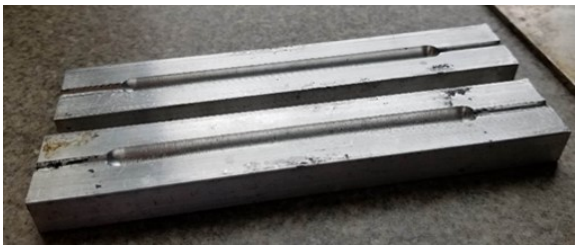

Figure 4.4: Mold for compression molding polyethylene tube specimens.

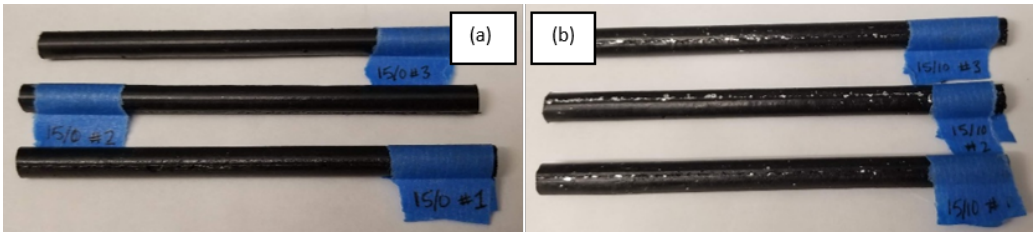

Figure 4.5: Conductive polyethylene specimens with (a) 15% carbon black (b) 15% carbon black and 10% aluminum.

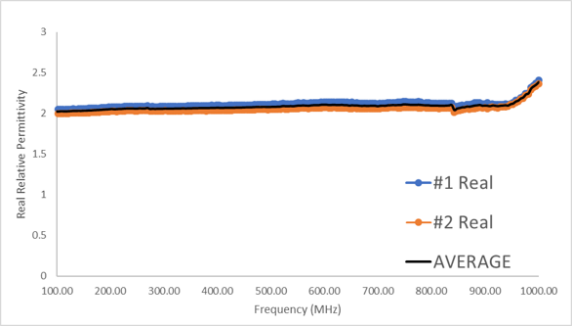

Figure 4.6: Real permittivity of neat polyethylene specimens.

these values are compared to the values for air in the same specimen holder. Figure 4.6 shows the relative permittivity of a neat polyethylene specimen over the range from 100 MHz to 1 GHz, which are common frequencies used with ground penetrating radar. This data agrees with tabulated values for the dielectric properties of polyethylene. Figure 4.7 shows the measured relative permittivity of conductive polyethylene specimens with 15% carbon black, and Figure 4.8 shows the measured relative permittivity for conductive polyethylene specimens with 15% carbon black and 10% polyethylene. Other studies on dielectric properties of conductive composites do not show the same frequency-specific peaks that can be seen in Figure 4.7 and Figure 4.8. Future work will determine the causes of these peaks in permittivity and a solution to remove them.

4.2.1 Doped Polyethylene Antennas

Once the 15-10 polyethylene was chosen as the target material, an antenna was molded from that material and compared to similar antennas made from steel foil. The results are shown in Figure 4.9. The largest response is generated by a cross

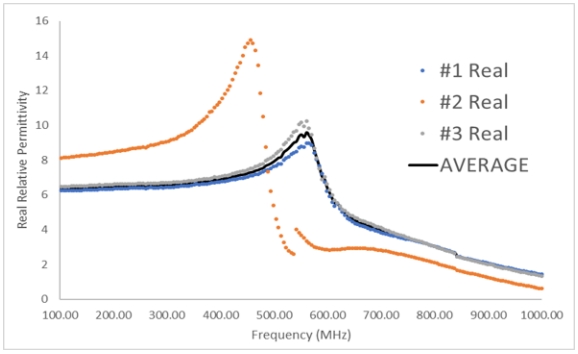

Figure 4.7: Real permittivity of polyethylene specimens with 15% carbon black.

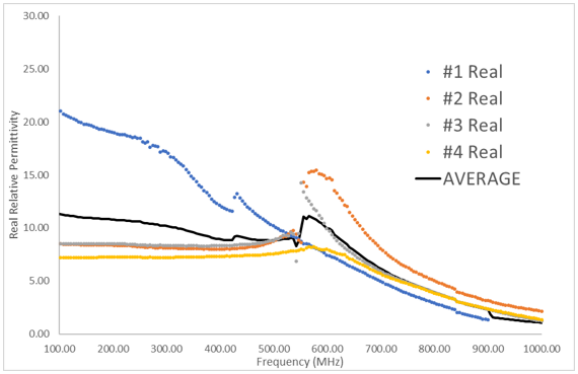

Figure 4.8: Real permittivity of polyethylene specimens with 15% carbon black and 10% aluminum.

polarization antenna, which is the antenna that is more ideal for this use. The next highest response comes from a double steel foil bowtie antenna, then a single steel foil bowtie antenna, then a doped polyethylene antenna. The blue response line at the bottom is the response generated by a polyethylene pipe. The response from the doped polyethylene antenna is not as strong as the identical antenna made from steel, which is to be expected given that the resistivity of steel is several orders of magnitude lower than that of the doped polyethylene. However, the response from the doped polyethylene antenna can still clearly be seen above the baseline response of the pipe.

This antenna test was designed as a proof of concept test, and so further work on the dimensions of the antennas should be done to get the strongest response from an antenna. Additionally, the antennas used for this test would fit on 4" main lines, but not the smaller 1" pipes that run to individual houses, so smaller antennas will have to be designed. The size of the antenna, primarily the length, affects the wavelength that it reflects, so a similar test will have to be repeated for the various sizes of antennas.

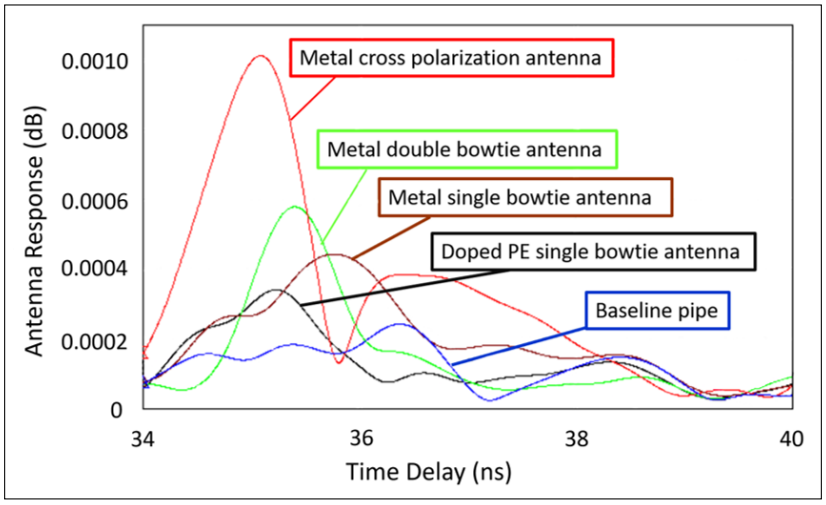

Figure 4.9: Response of antennas tested with a ground penetrating radar setup. The vertical axis is normalized strength of response.

4.3 Mechanical Property Characterization

Polyethylene pipes are manufactured through extrusion, and then pipes with diameters of 6" or less are coiled onto spools for storage and transportation. Because polyethylene has high ductility, the majority of pipe bending is done through cold working in the field. Coiling and straightening, as well as the process of installation, introduces strains in the polyethylene pipe. Polyethylene pipe can often achieve strains of 25-30% before local buckling occurs, though in practice is often limited to deformations of 7.5% or less for safety. Antennas attached to pipes prior to installation will experience the same strains as the pipes during service. In addition to requisite electromagnetic properties, the conductive polyethylene will need sufficient mechanical properties to survive the strains experienced by the pipe in service. The addition of high concentrations of filler materials into the polyethylene will alter the mechanical

properties of the material as well as its electromagnetic properties, so the mechanical properties of the material as well as the effect of the antennas on the pipe should be quantified. Specimens were created from unaltered polyethylene and the polyethylene modified with 15% carbon black and 10% aluminum flake that was used in the antenna experiments. To simulate the behavior of a doped polyethylene antenna molded to the outer surface of a polyethylene pipe, specimens were created with a layer of conductive polyethylene molded onto a neat polyethylene substrate. For these specimens, the ratio of the thicknesses was varied so that for some specimens, the antenna layer was very thin, and for others, the antenna layer comprised the majority of the thickness. Wires were molded into the bilayer specimens so that resistance across the specimens could be measured. To manufacture the specimens, a custom router fixture was created where the beams were fixed with a pin, allowing the ends of the fixture to remain open to allow for the wires in the specimen. This router fixture can be seen in Figure 4.10.

Specimens of all materials were tensile tested according to the procedure outlined in ASTM Standard D 638. Representative results and typical failure behavior for each material can be seen in Figure 4.11. Neat polyethylene can draw to several times its own length under tension and exhibits an extremely ductile fracture surface, as seen in Figure 4.11(c). However, the high concentrations of filler materials in the conductive polyethylene restrict its ability to draw, resulting in brittle failure behavior at much lower strains as seen in Figure 4.11(b). When the antenna material is molded to the pipe material, brittle fracture which begins in the doped polyethylene layer can propagate quickly into the neat polyethylene layer, resulting in brittle

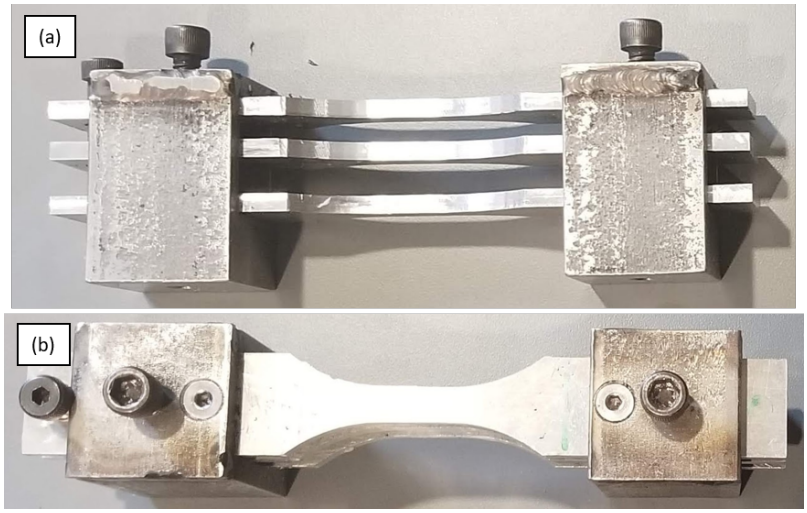

Figure 4.10: (a) Side view of router fixture. (b) Top view of router fixture.

failure in the neat polyethylene layer. The sharp decrease in the bilayer curve in the stress plot in Figure 4.11(a) represents brittle fracture which propagates through the majority of the cross sectional area of the specimen. Some tendrils of neat polyethylene remain, however, and drawing of these tendrils is the gradual decrease in the stress plot after mechanical failure. Evidence of the failure propagation is shown in Figure 4.11(d), which is a typical cross section of a fractured bilayer test specimen. Figure 4.11(e) shows the failure behavior of the neat polyethylene side of a bilayer specimen. Evidence of some drawing can be seen around the edges of the specimen, but most of the drawing has been restricted by the fracture propagation from the conductive side of the material.

In the case of conductive polyethylene antenna structures molded onto polyethylene pipes, this rapid crack propagation means that any damage which occurs to the antenna due to its lower strain to failure could be propagated through to the pipe,

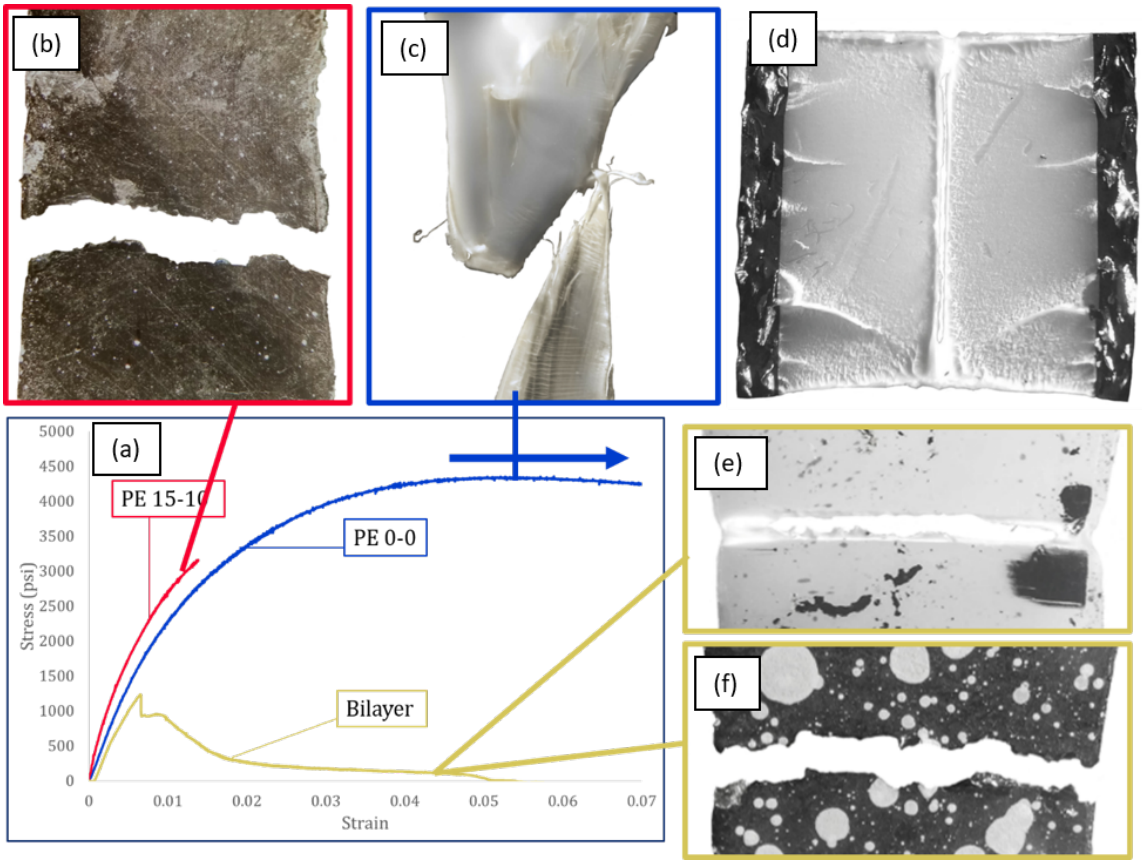

Figure 4.11: (a) Stress-strain graphs for conductive polyethylene, neat polyethylene, and bilayer specimens. (b) Fracture behavior of conductive polyethylene. (c) Fracture behavior of neat polyethylene. (d) Fracture surface of a bilayer specimen. (e) Fracture behavior of the neat layer of polyethylene in a bilayer specimen. (f) Fracture behavior of the conductive layer of polyethylene in a bilayer specimen.

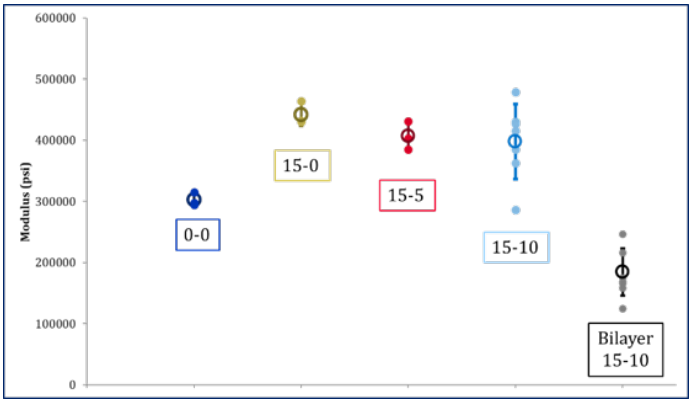

Figure 4.12: Elastic modulus for neat polyethylene, varying conductive polyethylenes, and bilayer polyethylene specimens.

causing damage to the pipe. Some methods for reducing fracture propagation between the materials have been studied, and future work on this project will attempt to further reduce damage propagation. Experimentally measured elastic modulus for all specimens is shown in Figure 4.12. The presence of carbon black and aluminum, two stiff materials, in the conductive polyethylene resulted in an increase in stiffness. As the amount of aluminum flake in the composite increased, the stiffness of the material did not increase, but the amount of scatter within each dataset did, indicating that the aluminum flake within the material can act as void content rather than reinforcement. The bilayer specimens had a lower effective modulus than any of the single material specimens.

Failure strains for all tested specimens are shown in Figure 4.13. Typically, the failure strain for neat polyethylene is defined at fracture, but because pipes used in industry are limited to strains below the drawing, failure strain was taken at the onset of drawing within the polyethylene. As expected from the failure behavior, adding such high quantities of carbon black to the composite results in a brittle

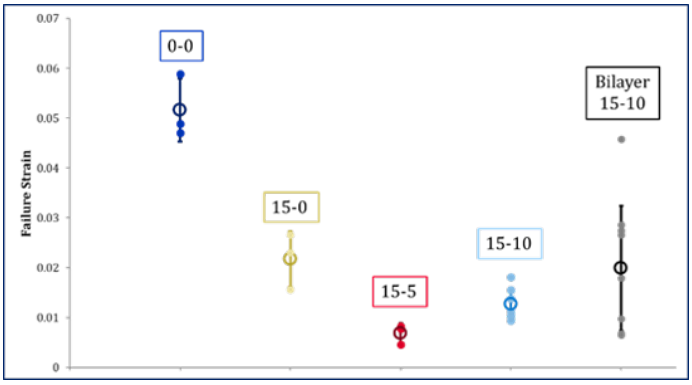

Figure 4.13: Failure strain for neat polyethylene, varying conductive polyethylenes, and bilayer polyethylene specimens.

material with much lower strains to failure than the neat polyethylene.

Strain to failure for the bilayer specimens showed high variance. Figure 4.14 shows the modulus and failure strain for each bilayer specimen compared to the relative thickness of the conductive polyethylene layer in that specimen. For instance, a specimen with equal layers of conductive and neat polyethylene would have a thickness ratio of 0.5. As seen in Figure 4.14, both elastic modulus and failure strain were highly dependent on the thickness ratio of the conductive polyethylene layer. As the thickness of the conductive polyethylene increases, the effective modulus of the composite increases, but the strain before fracture of the composite decreases. In the case of an conductive polyethylene layer molded to a neat polyethylene pipe, the ideal antenna would be as thin as possible to reduce the chance of damage to the pipe due to fracture in the antenna.

During tensile tests of the bilayer specimens, resistance was measured across the specimens to determine the point of electrical failure in the specimen. A schematic view of the bilayer specimens can be seen in Figure 4.15.

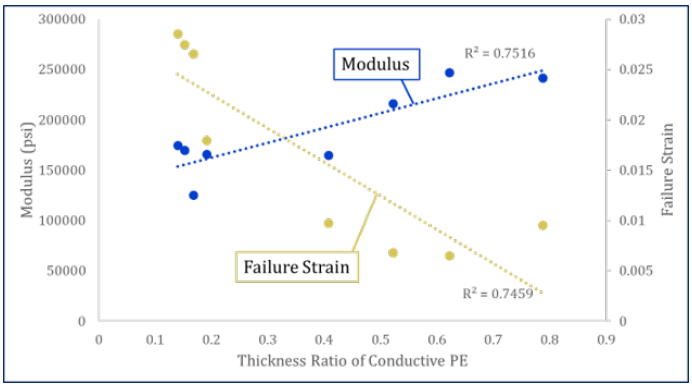

Figure 4.14: Modulus (blue) and failure strain (yellow) for bilayer specimens vs the relative thickness of the electroactive polyethylene layer.

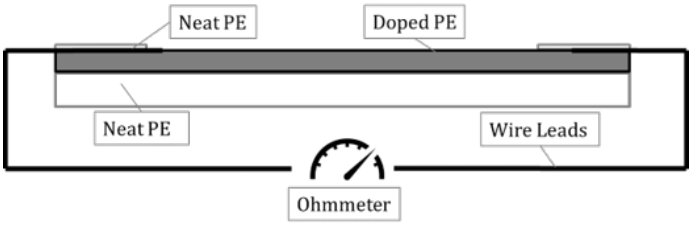

Figure 4.15: Schematic view of the cross-section of a bilayer tensile specimen.

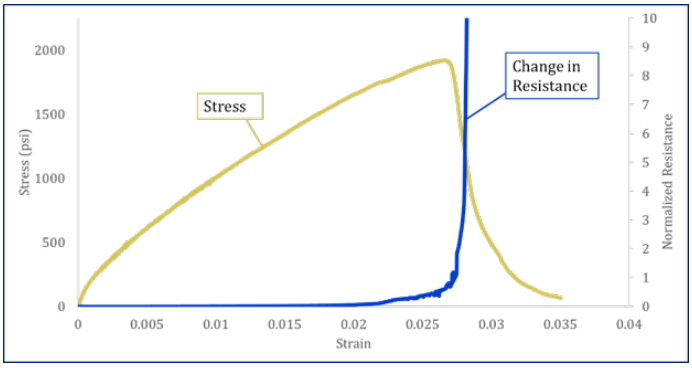

Figure 4.16: Stress vs strain and change in resistance vs strain for a bilayer specimen in a tensile test.

A typical graph generated by this experiment includes both strain and normalized change in resistance plots, as shown in Figure 4.16. The electrical failure strain, or the strain at which the normalized change in resistance increases to infinity, occurs after the mechanical failure strain, which occurs when the two halves of the test specimen fracture and can no longer carry a load. Though the two halves of the specimen are no longer mechanically able to carry a load, the small distances between the specimen halves are bridged by the aluminum flake, allowing current to still pass through. For a polyethylene antenna molded to a pipe, this is advantageous, as antennas which had sustained minor crack damage while attached to the antenna should still be able to function as intended.

Two of the specimens tested were loaded to over 1000 psi, then released, and then tested to failure. During the tensile test, one of these specimens, which had been loaded to 1700 psi, exhibited multiple cracks forming throughout the doped section and drawing in the neat section. Cracks in the doped material likely began forming during the preload, but because the specimen was released from strain

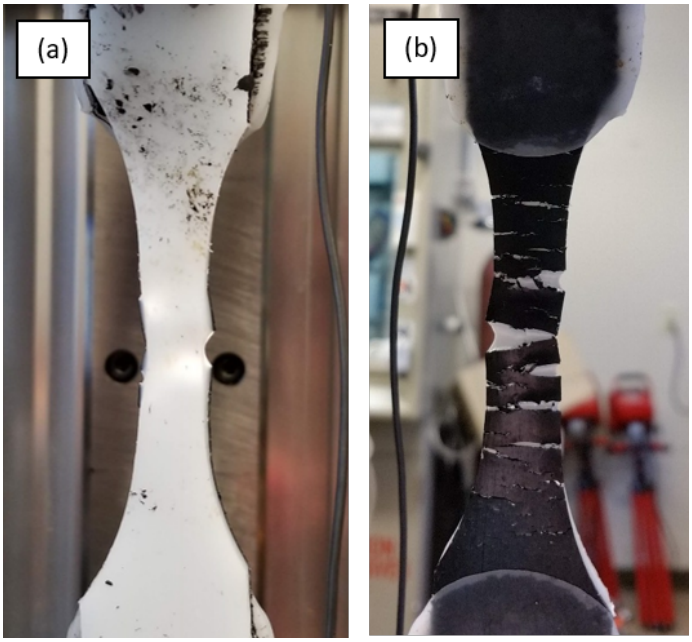

Figure 4.17: Gauge lengths of (a) the neat polyethylene layer and (b) the doped polyethylene layer of a bilayer tensile specimen that experienced drawing.

prior to fracture, the fracture energy could not propagate through the neat layer, allowing the plastic deformation to happen more similar to the typical behavior of neat polyethylene. This specimen during the tensile test is shown in Figure 4.17. The second specimen, which had been loaded with a lower stress of 1400 psi during the preload, failed in a brittle manner similarly to the other specimens.

Further testing will be done to determine a repeatable method, either with a certain stress or a low-cycle fatigue loading, through which the cracks in the doped layer could be created, reducing the chance of brittle fracture through the neat polyethylene. In the case of doped polyethylene antennas applied to polyethylene pipes, a brittle fracture in an antenna could propagate into the pipe and cause the pipe to fail, but a pre-cracked antenna would allow the polyethylene pipe to behave

normally. However, it must be determined if the existence of the pre-cracks in the material will have an adverse effect on either the electrical or mechanical properties of the material.

4.4 Specimen and SEM Imaging

4.4.1 Tensile Tests

After testing, the fracture surfaces of the specimens were examined with an optical microscope. A representative test specimen can be seen in Figure 4.18. The fracture surface of these specimens exhibited brittle behavior, with none of the drawing present in neat polyethylene tensile specimens.

Figure 4.19 shows images from a representative 15% CB-10%Al sample; Figure 4.19 shows an aluminum flake that is not bonded to the matrix and a valley in the polyethylene where an aluminum flake had been pulled out.

4.5 Bilayer Tensile Tests

During the bilayer tensile tests, when the doped polyethylene layer fractured, the crack would propagate through the neat polyethylene layer. In the case of a doped polyethylene antenna molded on to a neat polyethylene pipe, if the antenna were to crack while the pipe was in service, the crack could propagate through the pipe and cause damage.

The interface of the doped and neat layers of a bilayered polyethylene tensile

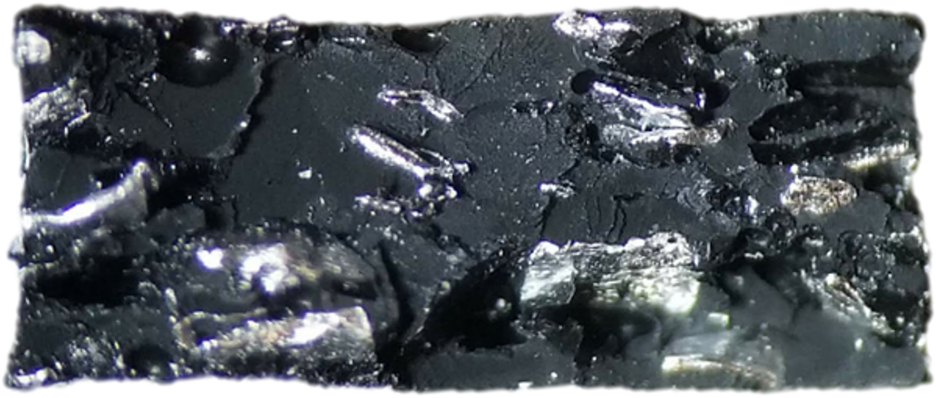

Figure 4.18: Fracture surface of a doped polyethylene tensile specimen.

specimen was examined with a scanning electron microscope. At higher magnification, it was apparent that the two layers were well bonded together. Figure 4.20 shows a section of the fracture surface where the difference between the materials can be easily seen. Ridges in the neat polyethylene layer originated from cracks in the doped polyethylene around the locations of aluminum flake.

Figure 4.21 shows high magnification images of the polyethylene fracture surfaces. In Figure 4.21, the material shown on the upper left of the image in the neat polyethylene, which exhibits some drawing, although it is still much more brittle than would be expected from just neat polyethylene. The lower right section of the image is the doped polyethylene, which does not show any signs of drawing. The two layers appear to be well bonded together across the entire width of the specimen.

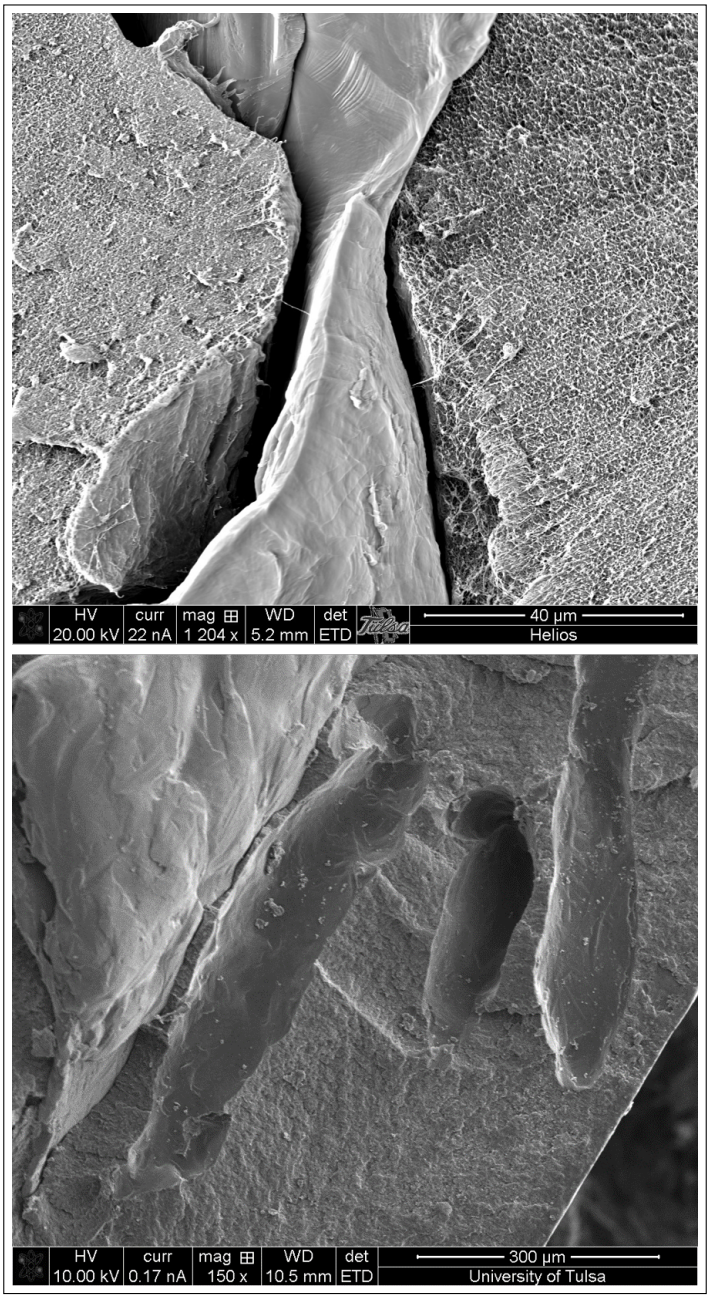

Figure 4.19: SEM images of the fracture surface of a polyethylene composite tensile specimen with 15% carbon black and 10% aluminum. (Top) An aluminum flake in the center, with doped polyethylene fracture surface on the left and right. Note the smooth texture of the aluminum relative to that of the polyethylene. (Bottom) Valleys in a doped polyethylene matrix where an aluminum flake has been pulled out. Note that the surface inside the valley is smooth like that of the aluminum.

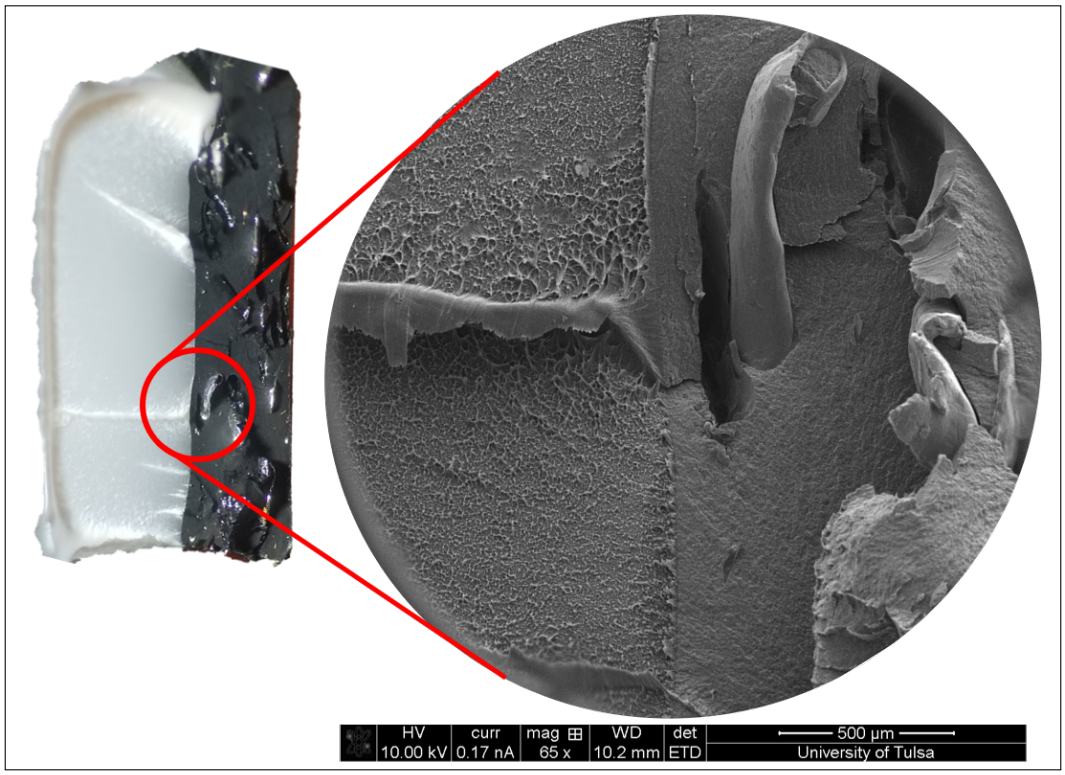

Figure 4.20: Fracture surface of a bilayer tensile specimen as seen with a scanning electron microscope.

Antennas molded to polyethylene pipe in this manner would remain attached to the pipe, preventing shifting of the radar target away from the pipe while in the ground, which is the case with tracer wires.

In order for these doped polyethylene antennas to become commercially viable, the tendency for fracture to propagate through both layers of the material will have to be reduced. A layer of another material which bonds to polyethylene less well could be added between the two materials to slow the advancement of the crack. Another method involves pre-cracking the doped polyethylene layer through fatigue. The presence of many small cracks in the material will prevent one large crack from forming and propagating through the neat polyethylene layer, though this might adversely affect the electrical properties of the antenna.

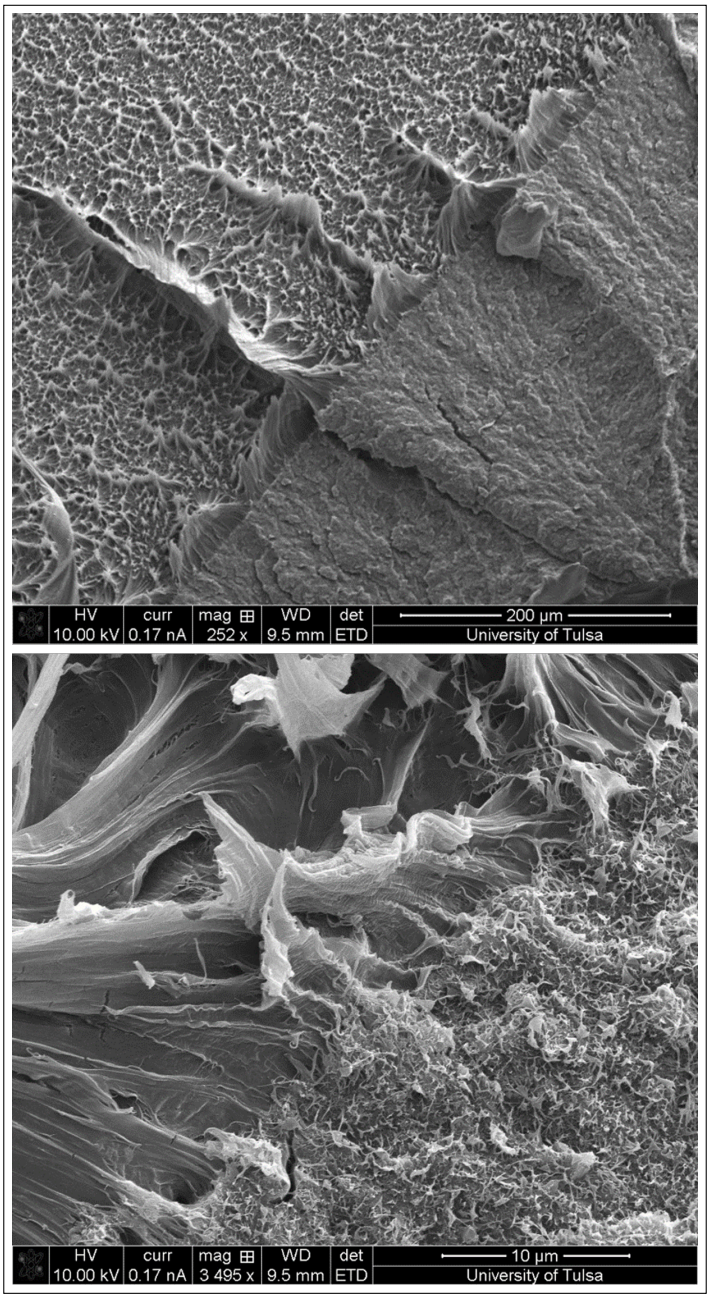

Figure 4.21: SEM images of the fracture surface of a doped and neat polyethylene composite tensile specimen. In both images, the neat polyethylene is in the upper left of the image and the doped polyethylene is in the lower right. (Top) 250x (Bottom) 3500x

4.6 Fracture Toughness

Fracture toughness for the neat and doped polyethylene specimens is shown in Figure 4.22. The doped polyethylene exhibits behavior that is more brittle than the neat polyethylene, although the difference between the two materials is not statistically significant. The doped polyethylene should have similar resistance to crack growth as the neat polyethylene. However, the aluminum flakes in the doped polyethylene cause the presence of large cracks in the doped polyethylene that do not exist in the neat polyethylene, which lead to the shorter strain to fracture seen in the doped and bilayer specimens.

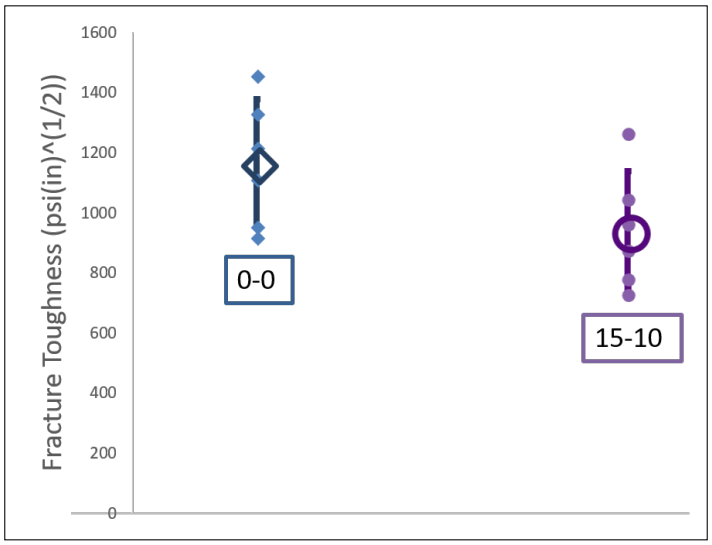

Figure 4.22: Fracture toughness of both neat and doped polyethylenes.

After fracturing, the crack lengths of the fracture surfaces were measured to ensure that the test was valid according to the requirements of the standard. Representative fracture surfaces for both neat and doped polyethylene three point bend test specimens

are shown in Figure 4.23.

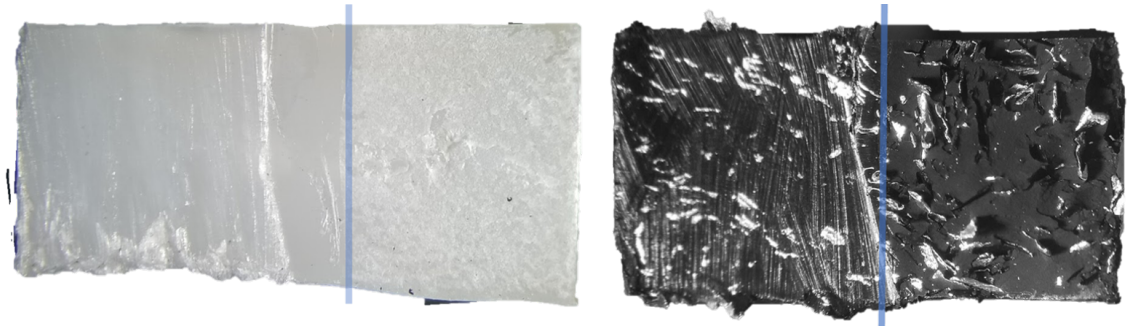

Figure 4.23: Fracture surfaces of three point bend test specimens. For each specimen, the precut area is to the left of the blue line and the fractured area is to the right. (Left) Neat (Right) Doped

4.7 Pipe Strain and DIC

It is important to understand the strains that a pipe will experience in service to design an antenna that can function at those same strains. Digital Image Correlation was used to measure the strains on a pipe bent to radii that would be seen in service. A representative output from the DIC software can be seen in Figure 4.24. An area of interest was chosen at the outer surface of the pipe near the fixed end where the rigid body displacement of the pipe was smaller. The points in this area were averaged to find the strain value for the pipe at each bend.

Figure 4.25 shows the calculated strains for a 1" pipe bent over a constant radius, with the corresponding strains calculated using DIC. The average measured failure strain for the doped 15-10 polyethylene is overlayed on the graph. At lower radii, the strain experienced by the pipe is less than the failure strain of the material, but at

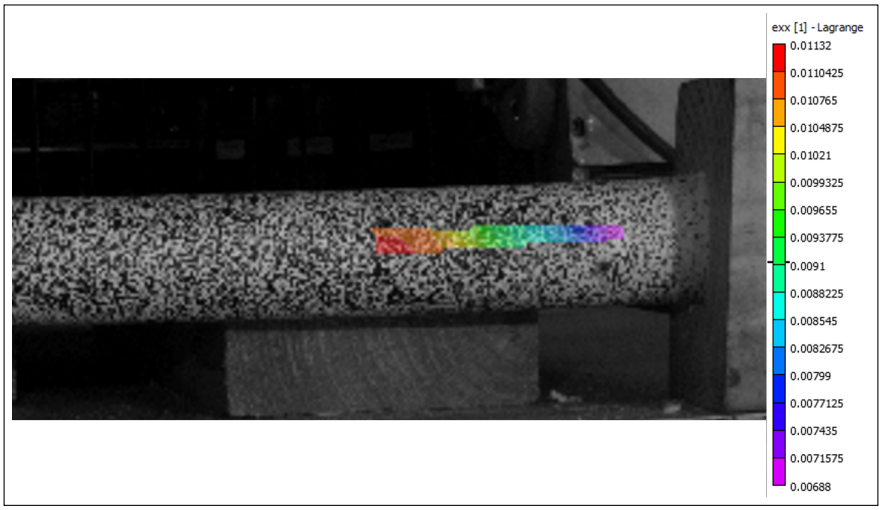

Figure 4.24: DIC results for the pipe bend test with a constant mandrel with a radius of 17".

the tighter short term radius, the antennas would likely sustain some damage caused by the higher strains.

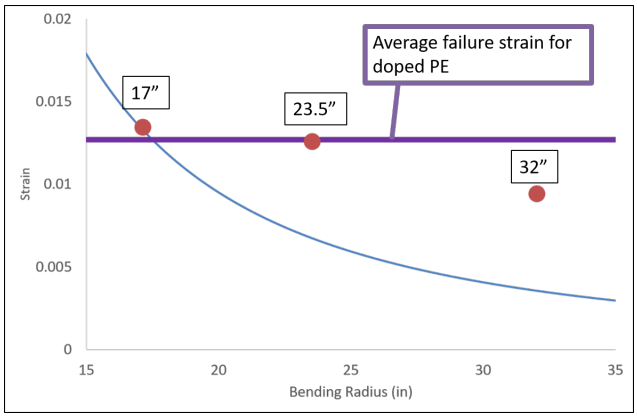

Figure 4.25: Measured and calculated strains for a 1” pipe in bending over a constant radius mandrel. The failure strain for the 15-10 doped polyethylene is overlayed.